

Morphological study and photo-addressing in poly(styrene-*b*-butadiene-*b*-styrene) block copolymers with azobenzene groups and polystyrene matrix: influence of chemical bonding

Raquel Fernández, Iñaki Zalakain, José Angel Ramos, Loli Martín, Iñaki Mondragon*

'Materials + Technologies' Group, Department of Chemical & Environmental Engineering, Polytechnic School, Universidad País Vasco/Euskal Herriko Unibertsitatea, Plaza Europa 1, 20018 Donostia-San Sebastián, Spain.

* Corresponding author. Tel.: +34 943 017 177; fax: +34 943 017 130.

E-mail address: inaki.mondragon@ehu.es (I. Mondragon)

ABSTRACT

The main goal of this work was the synthesis of new azo-functionalized block copolymers (BCP) from epoxidized poly(styrene-*b*-butadiene-*b*-styrene) modified with azobenzene groups by one-step facile reaction between the epoxy groups and an azo-amine. The epoxy/amine reaction was verified by Fourier transform infrared spectroscopy. Additionally, we studied the effect of covalent attachment of the azobenzene moieties by analyzing the morphology and the optical anisotropic response of the resulting azo-containing BCP, with respect to solution mixing of the azobenzene as a guest in the BCP host without chemical bonding. Self-assembly of all modified BCP resulted in phase-separated morphologies on the nanometer scale. Nonetheless, segregation of azobenzene aggregates onto the BCP surface was observed in guest-host systems. In relation to the optical anisotropic behaviour of the resulting materials, two distinct optical responses were observed depending on the existence or not of covalent attachment of the azo-chromophores to the BCP.

Keywords: block-copolymer; epoxy; azobenzene; microstructure; birefringence

INTRODUCTION

The introduction of photo-chromic groups in polymers is very attractive as it offers the opportunity of generating new light-sensitive materials and optical devices [1]. In particular, polymers with azobenzene units or azo-polymers have been widely investigated because of their potential applications in optical recording processes based on the photo-orientation of the azo-chromophores through polarised light induced *trans-cis-trans* isomerisation cycles [2-8]. Most studies on this subject have been performed with amorphous and liquid crystalline azo-containing homopolymers and random copolymers. However, recently, the development of block copolymers (BCP) containing azobenzene units has gained importance [9-25]. It is well-known that BCP can form microphase separated nanostructures with cylindrical, lamellar, spherical or bicontinuous morphologies [26-32]. The confinement of photo-responsive units in nanosized block copolymer domains gives these materials unique properties, because of the possibility of altering their self-assembly behaviour, while allowing the incorporation of molecules with optical features. Additionally, the reorientation of nanosized domains themselves, induced by the irradiation of this type of polymers, has also been reported. In particular, Ikeda and co-workers [33] demonstrated a molecular cooperative motion between azobenzene moieties and other photo-inert groups in azo-containing BCP with specifically designed structures. The azo-chromophores became aligned, triggered by the irradiation with a polarized laser beam at 488 nm, and the photo-inert groups were oriented together with the azobenzenes by supramolecular cooperative motions, although they did not absorb the actinic light.

The applications related to holographic optical storage are of the most interesting for researchers [34, 35]. To fully exploit the advantages of holography, thick films of tens or hundreds of microns are needed. Nevertheless, it is normally limited to azo-

polymer thin films since, due to the optical absorption of azobenzene moieties in the wavelength region of the recording light, thick films of azo-homopolymers cannot be illuminated through the complete film thickness. To decrease the optical absorption, the azobenzene content has to be diluted. This can be achieved by copolymerisation of the azo-chromophore with other monomer that does not absorb at the excitation wavelength. However, it has been verified that random azo-copolymers show a lower photo-induced response with respect to that of the corresponding azo-homopolymers. This fact has been associated with a decrease of interactions among azobenzene moieties, as a consequence of their statistical distribution in the polymeric chain. In an attempt to obtain an azobenzene dilution while keeping those interactions among azobenzenes, BCP with an azo-block having the same composition as the homopolymer and another block that does not absorb light in the photo-excitation region can be used. Depending on molecular weight and composition, block segregation appears in such a way that a microstructure of azobenzene domains in the diluting polymer can be induced. Thus, a decrease of the azobenzene content is achieved while a photo-induced response of the azo-block similar to that of the homopolymer can be expected [36].

Moreover, one of the most important parameters of holographic gratings is the diffraction efficiency (DE). Azo-block copolymers are good candidates to control the DE by surface relief grating enhancement upon microphase separation. Compared with other methods to control the DE, such as mechanical stretch, electrical switch, ..., the microphase separation method has the advantage of being simple and convenient. That is to say, holographic gratings can be inscribed at room temperature and subsequent annealing improves the DE by almost two orders of magnitude [37, 38]. These holographic gratings with enhanced effect might be applied to secure information storage since the information can be easily read out by the thermally induced

microphase separation [39].

Based on that knowledge, combining the excellent properties of azo-polymers with microphase separation, azo-block copolymers might find diverse uses in advanced technology as well as newly promising nanotechnology. However, the development of well-defined nanostructures involves the synthesis of BCP with controlled macromolecular architecture, molecular weight distribution, and composition. Several polymerization methods, such as anionic, cationic, free radical and metal-catalyzed polymerizations, have been explored to build azo-containing BCP that meet these requirements [39]. Alternatively, we present here the functionalization via epoxidation of commercial BCP, based on poly(styrene-*b*-butadiene-*b*-styrene) (SBS), modified with azobenzene moieties by one-step facile reaction between the epoxy and azo-amine groups. This is a novel and simple way of preparing azo-functionalized block copolymers as well as very versatile considering that the epoxy group is receptive to a wide range of reagents. Therefore, this functional group can react with different kinds of chromophores with electron-donor groups containing hydrogen, such as amines, amides, acids, anhydrides, phenols, ..., giving rise to a large variety of azo-containing BCP, taking into account also the great diversity of commercial available SBS type copolymers. In addition, we investigate the influence of covalent attachment of the azobenzenes by studying the morphology and photo-addressing behaviour of the resulting azo-containing BCP, with respect to solution mixing of the azo-chromophores without chemical bonding as guest-host systems.

EXPERIMENTAL

Materials

An azo-chromophore, 4-(4-nitrophenylazo)aniline ($(\text{O}_2\text{N})(\text{C}_6\text{H}_4)\text{N}=\text{N}(\text{C}_6\text{H}_4)(\text{NH}_2)$), Disperse Orange 3 (DO3), with a melting temperature of 200 °C, was supplied by Aldrich. Two SBS linear triblock copolymers, C500 and C540, with 30 and 40 wt % of polystyrene (PS), respectively, were kindly supplied by Repsol-YPF. Gel permeation chromatography (GPC) was performed with a Perkin-Elmer LC-295 chromatograph. The mobile phase was tetrahydrofuran (THF) at flow rate of 1 mL·min⁻¹. The number-average molar masses (M_n) were 102,000 g·mol⁻¹ for C500 and 75,000 g·mol⁻¹ for C540 as calculated using a universal calibration method with polystyrene standards. PS homopolymer was purchased from Polymer Source and had a M_n of 20,800 g·mol⁻¹ as given by the manufacturer. All materials were used as received without further purification.

Synthesis of photo-addressable block copolymers

Different epoxidized SBS triblock copolymers, C500epX or C540epX (X being the degree of epoxidation (mol %) with respect to PB double bonds), were obtained by epoxidation of PB-blocks. This reaction was carried out using hydrogen peroxide in the presence of an *in situ* prepared catalyst system in a water/dichloroethane biphasic mixture, following a procedure described elsewhere [40]. Then, the resulting epoxidized copolymers were reacted with the azo-amine, DO3, in stoichiometric ratios, between epoxy groups and active hydrogens of the amine, at 110 °C during 24 h under vacuum conditions. Figure 1 shows a schematic illustration of the synthesis procedure followed. In addition, guest-host systems of C500 and C540 containing DO3 (C500-DO3 and C540-DO3) and PS (C500-DO3-PS and C540-DO3-PS) were also prepared.

All samples have similar amounts of azo-chromophore on the order of 15 (\pm 2) wt %.

Films preparation

Films of the azo-block copolymers and the guest-host systems were prepared by spin-coating from 5 wt % solutions in THF:dichloroethane 0.15:0.85 using a P6700 spin-coater from Cookson Electronics. The spinner program was 1000 rpm for 60 s. Residual solvent was removed by evaporation at room temperature. Then, films were annealed at 110 °C during different times, 24 and 48 h, under vacuum. The films thicknesses were determined by ellipsometry using a Semilab Sopra GES-5E ellipsometer from Telstar.

Techniques

High resolution ^1H NMR spectra, recorded in deuterated chloroform solution with a Bruker 300 MHz spectrometer at 25 °C, were used to determine the degree of epoxidation. ^1H NMR chemical shifts were measured with respect to tetramethylsilane (TMS) as internal standard.

Differential scanning calorimetry (DSC) was performed using a Mettler Toledo DSC 192 822 differential scanning calorimeter equipped with a sample robot 193 TSO 801 RO. Nitrogen was used as purge gas (10 mL \cdot min $^{-1}$). The reaction temperature and the glass transition temperature (T_g), defined as the onset of the change in specific heat, were determined from the thermograms obtained in heating scans at 10 °C \cdot min $^{-1}$.

Infrared spectra were taken using a Nicolet Nexus 670 Fourier transform infrared (FTIR) spectrometer equipped with a single horizontal golden gate attenuated total reflectance (ATR) cell. Spectra were recorded using a spectral width ranging from 600 to 4000 cm $^{-1}$, with 2 cm $^{-1}$ resolution and an accumulation of 20 scans.

The morphology of the samples was studied by atomic force microscopy (AFM). AFM images were obtained with a Nanoscope IIIa scanning probe microscope (Multimode™, Digital Instruments). Tapping mode (TM) in air was employed using an integrated tip/cantilever (125 μm in length with *ca* 300 kHz resonant frequency). Typical scan rates during recording were 0.7-1 line·s⁻¹ using a scan head with a maximum range of 16 x 16 μm.

Optical storage experiments were carried out at room temperature and under ambient conditions. The experimental setup used was similar to that previously reported [41]. Optical birefringence was induced in films of the azo-block copolymers and the guest-host systems using a linearly polarized argon laser operating at 488 nm (writing beam) with a polarisation angle of 45° with respect to the polarisation direction of a low power He-Ne laser operating at 632.8 nm (reading beam). The power of the writing beam used in the experiments was varied between 6 and 20 mW on a spot of 0.4 mm² and the change in the transmission of the reading beam, which passed through the sample between two crossed polarisers, was measured with a photodiode. The induced birefringence (Δn) was determined by measuring the reading beam transmission ($T = I/I_0$) according to:

$$\Delta n = (\lambda/\pi d) \sin^{-1} (I/I_0)^{1/2}$$

where λ is the wavelength of the reading beam, d is the film thickness, I is the intensity of the reading beam after the second polariser and I_0 is the transmitted intensity of the reading beam between parallel polarisers in absence of anisotropy.

RESULTS AND DISCUSSION

A brief account of the characteristics of the modified copolymers can be found in Table 1. ¹H NMR spectra provided evidence for the existence of reactive epoxy

groups in PB-block chains. Figures 2a-d show ^1H NMR spectra of the parent copolymers, C500 and C540, and the epoxidized copolymers, C500ep11 and C540ep14. C500 and C540 showed two signals at 5.03 and 5.45 ppm, corresponding to the olefinic protons of 1,2- and 1,4-butadiene units. The corresponding epoxidized copolymers showed likewise two new signals attributed to the protons attached to *trans*- and *cis*-epoxy groups at 2.70 and 2.96 ppm, respectively. The degree of epoxidation was calculated by the integration of these new signals compared to the sum of the intensities of double bond proton peaks.

Firstly, the reaction between the epoxy groups and the azo-amine was investigated. Thermal behaviour of C500ep11-DO3 and C540ep14-DO3 was studied by differential scanning calorimetry. Dynamic DSC scans (not shown here) were utilized to estimate reaction temperatures and T_g values of samples. According to this study, 110 °C during 24 h was selected as reaction condition for both systems. In order to verify the complete reaction of reactants, isothermal DSC scans (not shown here) were obtained at that experimental condition (110 °C, 24 h). In a subsequent DSC scan in dynamic mode no residual heat of reaction was seen, proving total reaction. In addition, the synthesis of both azo-block copolymers, C500ep11-DO3 and C540ep14-DO3, was carried out under vacuum to avoid possible oxidation reactions.

To corroborate the epoxy groups reaction, FTIR spectra in the mid IR region of the samples were also obtained. In Figures 3a-b the spectra of DO3, C500ep11-DO3 and C500ep11 with and without annealing, at 110 °C for 24 h under vacuum, are plotted. The main infrared absorption bands of these samples are listed in Table 2. The bands associated with C-O-C groups for *trans*- and *cis*-1,4-epoxidized copolymer appeared at 890 and 814 cm^{-1} , respectively. The corresponding band for 1,2-epoxidized units should appear around 911 cm^{-1} . It is worth noting that PS and 1,2-PB have a

characteristic band at 910 cm^{-1} . These bands are too close to the C-O-C group for 1,2-epoxidized copolymer and, thus, it is hard to distinguish them [40]. As can be observed, total disappearance of the band at 890 cm^{-1} occurred, confirming the complete reaction of epoxy groups. Furthermore, a decrease in intensity of the band at 1640 cm^{-1} , associated with the in-plane bending vibration of NH_2 groups, can also be noticed. Additionally, in order to determine the possible existence of secondary reactions, the spectrum of C500ep11 annealed at $110\text{ }^\circ\text{C}$ during 24 h under vacuum was also evaluated. A slight variation in the C-O-C groups band (890 cm^{-1}) can be seen, as well as the appearance of two new bands at 1712 and 3400 cm^{-1} associated with the stretching vibration of C=O and OH groups, respectively. These results would indicate the existence of secondary reactions as a consequence of the thermal treatment. Nonetheless, no sign of such reactions can be seen in C500ep11-DO3 spectrum, which could be an evidence that the addition of amine functional groups to epoxy is the main and most favoured reaction. Similar results were obtained for C540ep14 and C500ep14-DO3.

The samples morphologies, generated by self-assembly of the block copolymers, were investigated using TM-AFM. In order to obtain repeatable results, different areas of the films were scanned. Taking into account the resemblance of height and phase TM-AFM images of each sample, only phase images are shown. In Figure 4 TM-AFM phase image and profile of the guest-host system C500-DO3 after annealing at $110\text{ }^\circ\text{C}$ for 24 h under vacuum can be observed. This block copolymer shows a self-assembled cylindrical structure after the annealing treatment. In particular, most of PS cylinders are positioned parallel to the continuous phase of PB-block. Nevertheless, some of them perpendicular to the surface of PB-block domains can also be observed. In addition, three different scale colours can be seen in the image: PS-block domains appear brighter

than PB-block domains, since PS has a higher modulus than PB at room temperature. However, small azobenzene aggregates detected are the most rigid and, therefore, the brightest ones. Even though films preparation was made from homogeneous solutions, when solvents evaporated, migration of DO3 onto the BCP surface occurred. Based on the chemical structure of the azobenzene molecule, DO3 might have higher affinity for PS than for PB. To confirm this assumption, TM-AFM phase image and profile of a C500-DO3/PS homopolymer blend (C500:PS 80:20) were obtained (Figure 5). In this case, the annealing treatment was as follows: first, 110 °C for 24 h under vacuum and, then, 210 °C for 4 min. This system, C500-DO3-PS, shows a cylindrical morphology similar to that for C500-DO3, but macrophase separation of PS homopolymer can also be noticed as well as an increase of the PS cylinders size from ~ 35 to ~ 45 nm, as compared to C500-DO3 system, indicating that some PS homopolymer is miscible with PS-block. With regard to azobenzenes location, they are predominantly located over PS domains, as clearly inferred from TM-AFM image. What is more, azobenzene aggregates are preferentially segregated in PS homopolymer phase, thus demonstrating the higher affinity of the azo-chromophores for PS than for PB. Similarly, samples of C540-DO3 and C540-DO3-PS were studied using TM-AFM and segregation of DO3 onto the BCP surface was also observed.

The morphologies of the azo-containing BCP with the chromophores covalently linked, C500ep11-DO3 and C540ep14-DO3, were also analyzed by TM-AFM. Figure 6 shows images of the different morphologies generated after thermal treatment at 110 °C during different times, 24 and 48 h. The films were formed of a continuous phase of PB, where 11 or 14 mol % of PB is epoxidized, with microphase separated domains of PS. The employed epoxidation degrees do not modify the morphological features of the raw BCP but, though not shown, a higher epoxidation extent than that used in this work

produces significant changes. For C500ep11-DO3 (Figures 6a and 6c), with 24 h treatment, a cylindrical morphology was observed, where the PS cylinders orientation started to change from parallel to perpendicular, to finally situate nearly all perpendicular to the continuous phase surface with 48 h of annealing. Nonetheless, C540ep14-DO3 (Figures 6b and 6d) showed a similar morphology for 24 and 48 h of thermal treatment, with almost all PS cylinders oriented parallel to the surface. Here it should be pointed out that in none of these samples aggregation of azobenzene was detected. That is to say, thanks to the covalent attachment of the azo-chromophores to the BCP via addition reaction of DO3 amine groups to epoxy groups, completely homogeneous azo-containing block copolymers were achieved.

On the other hand, the optical anisotropic properties of all the BCP with azobenzene groups prepared were also evaluated. Optical anisotropy is a photo-induced birefringence in the polymeric films resulting from a reorientation of the azobenzene moieties. Generally, linearly polarized light is used to provoke a *trans-cis* isomerisation followed by a molecular reorientation and a *cis-trans* isomerisation. The absorption and reorientation sequence will be repeated until the azobenzene molecules dipole moment lies in a direction which is perpendicular to the polarisation direction of the writing beam. In this way, optical anisotropy can be induced in the films [43]. In Figures 7a-f writing-relaxing sequences obtained for films of different kind of systems with comparable DO3 amounts are plotted. In all cases, the reading beam continuously illuminates the samples. At the beginning of the experiment there is no transmission of the reading beam, as the azo-chromophores in *trans* form, which is the more stable configuration, are randomly distributed, the films being isotropic. At point *A*, the writing beam was turned on and the reading beam was transmitted through the polariser-sample-polariser system due to the optical anisotropy induced in the films as a

result of *trans-cis-trans* photo-isomerisations that led to the orientation of *trans* molecules perpendicular to the polarisation vector of the writing beam. In particular, different responses versus argon laser irradiation were seen. Guest-host systems (Figures 7a, 7b and 7c) and epoxidized SBS with DO3 previous thermal treatment (Figure 7d) showed similar behaviours. The photo-induced birefringence was rapidly built up to the saturation level but, when the writing beam was turned off at point *B*, Δn quickly fell off indicating the complete randomization of the azo-chromophores orientation. After annealing of epoxidized SBS with DO3 samples, a slow down of the azobenzenes orientation rate was noticed as well as a lower value of Δn . Representative examples of this behaviour are plotted in Figures 7e and 7f for C500ep11-DO3 and C540ep14-DO3, respectively, after thermal treatment at 110 °C during 24 h. Quantitatively, a maximum optical birefringence of just $\Delta n = 0.43 \cdot 10^{-2}$ was obtained. This result is probably due to the high molecular mobility at room temperature of the epoxidized PB-block with azobenzene, since its T_g is in the order of -55 °C for C500ep11-DO3 and -59 °C for C540ep14-DO3. It has to be taken into account that the saturated level of Δn is the result of a combination of two processes: photo-orientation, which increases birefringence, and thermal randomization, which decreases its level. These two processes reach an equilibrium state while illumination is on, and the preponderance of one or the other determines the saturated level [44, 45]. However, as was proven, the azobenzenes movement was somewhat restricted in the systems where they are covalently attached to the BCP from one end of the molecule, compared to the guest-host systems where the azo-chromophores have total freedom of movement. Additionally, for C500ep11-DO3 and C540ep14-DO3 after thermal treatment, when the writing beam was turned off (point *B*), Δn rapidly fell off initially, probably due to thermally activated dipole reorientation which would tend towards randomization of the

birefringence [46]. But, immediately after, it was observed that the relaxation process of the photo-induced orientation was also slower compared to the guest-host systems and C500ep11-DO3 without annealing, demonstrating once more the influence of chemical bonding. The effect of the writing power in the photo-induced birefringence was also analyzed. With that aim, films were irradiated with two different laser powers: 6 and 20 mW, as Figures 7a-c show. The level of achieved optical anisotropy was directly proportional to the number of photons involved in the writing process [43]. Thus, Δn was higher with 20 mW than with 6 mW of laser power. Nevertheless, differences in Δn values for both powers employed were small. This could be due to the fact that, as the laser power increased, the thermal effect could not be neglected since the heat from irradiation of writing beam was enough to increase the temperature around the irradiating point. This sample heating might counteract the orientation process, causing a decrease in Δn . In the case of azo-functionalized block copolymers, C500ep11-DO3 and C540ep14-DO3, a laser power of 20 mW was required in order to be able to obtain clear plots of optical responses.

CONCLUSIONS

Novel azo-functionalized block copolymers were satisfactorily synthesized. To achieve this goal two poly(styrene-*b*-butadiene-*b*-styrene) copolymers were first epoxidized through PB-block chains. The existence of reactive epoxy groups in PB-blocks was proven by ^1H NMR spectroscopy. Then, both epoxidized SBS block copolymers were reacted with an azo-amine in stoichiometric ratios at 110 °C for 24 h under vacuum to obtain two azo-containing block copolymers. FTIR was used to confirm the epoxy groups reaction. Total disappearance of the absorption band associated with epoxy groups was clearly observed.

Furthermore, the influence of covalent attachment of the azobenzene moieties was studied by analyzing the morphology of the resulting azo-functionalized BCP with respect to guest-host systems by TM-AFM. In all cases, a cylindrical structure after annealing treatment was generated by self-assembly of the block copolymers. Nevertheless, in guest-host systems aggregation of azobenzene units was detected onto the BCP surface. Specifically, it was verified that the azobenzene was predominantly distributed onto PS-block domains, probably thanks to its higher affinity for PS than for PB chains. With regard to the azo-functionalized BCP, azobenzene aggregates were not detected. Therefore, the covalent attachment of the azo-chromophores to the BCP via epoxy/amine reaction resulted in completely homogeneous azo-containing block copolymers.

The effect of covalent attachment of the azobenzene groups to the BCP over the optical anisotropic response was also studied. Two different behaviours were observed depending on the existence or not of covalent attachment of the azo-chromophores to the BCP. In summary, a slow down of the azobenzenes orientation rate as well as a lower value of birefringence was obtained for the azo-functionalized BCP as compared to the guest-host systems. The relaxation process of the induced orientation was also slower compared to the guest-host systems. This was probably due to the fact that the azobenzenes movement is somewhat restricted in the systems where they are covalently linked to the BCP from one end of the molecule, compared to the guest-host systems where they have total freedom of movement. Thus, this would reveal again the influence of chemical bonding.

The main advantages of this novel strategy to synthesize azo-containing BCP is its simplicity and versatility, opening up the possibility of designing a wide range of SBS type block copolymers with azobenzene groups.

ACKNOWLEDGEMENTS

Financial support from the Basque Country Government in the frame of Grupos Consolidados (IT-365-07), ETORTEK/inanoGUNE (IE08-225 and IE09-243) projects, and the Ministry of Education and Science for MAT2009-06331 project is gratefully acknowledged. The authors also thank the technical and human support provided by SGIker (Macrobehaviour-Mesostructure-Nanotechnology unit) (UPV/EHU, MICINN, GV/EJ, ESF).

REFERENCES

- [1] Hayakawa T, Horiuchi S, Shimizu H, Kawazoe T, Ohtsu M. Synthesis and characterization of polystyrene-*b*-poly(1,2-isoprene-*ran*-3,4-isoprene) block copolymers with azobenzene side groups. *J Polym Sci: Part A: Polym Chem* 2002; 40:2406-2414.
- [2] Kumar GS, Neckers DC. Photochemistry of azobenzene-containing polymers. *Chem Rev* 1989; 89:1915-1925.
- [3] Viswanathan NK, Kim DY, Bian S, Wei Liu JW, Li L, Samuelson L, Kumar J, Tripathy SK. Surface relief structures on azo polymer films. *J Mater Chem* 1999; 9:1941-1955.
- [4] Delaire JA, Nakatani K. Linear and nonlinear optical properties of photochromic molecules and materials. *Chem Rev* 2000; 100(5):1817-1846.
- [5] Natansohn A, Rochon P. Photoinduced motions in azo-containing polymers. *Chem Rev* 2002; 102:4139-4175.
- [6] Ikeda T. Photomodulation of liquid crystal orientations for photonic applications. *J Mater Chem* 2003; 13:2037-2057.
- [7] Yesodha SK, Sadashiva Pillai CK, Tsutsumi N. Stable polymeric materials for

- nonlinear optics: a review based on azobenzene systems. *Prog Polym Sci* 2004; 29:45-74.
- [8] Oliveira Jr ON, Dos Santos Jr DS, Balogh DT, Zucolotto V, Mendonça CR. Optical storage and surface-relief gratings in azobenzene-containing nanostructured films. *Adv Colloid Interf Sci* 2005; 116:179-192.
- [9] Moriya K, Seki T, Nakagawa M, Mao G, Ober CK. Photochromism of 4-cyanophenylazobenzene in liquid crystalline-coil AB diblock copolymers: the influence of microstructure. *Macromol Rapid Commun* 2000; 21:1309-1312.
- [10] Cui L, Tong X, Yan X, Liu G, Zhao Y. Photoactive thermoplastic elastomers of azobenzene-containing triblock copolymers prepared through atom transfer radical polymerization. *Macromolecules* 2004; 37:7097-7104.
- [11] Frenz C, Fuchs A, Schmidt H-W, Theissen U, Haarer D. Diblock copolymers with azobenzene side-groups and polystyrene matrix: synthesis, characterization and photoaddressing. *Macromol Chem Phys* 2004; 205:1246-1258.
- [12] Jiang J, Tong X, Zhao Y. A new design for light-breakable polymer micelles. *J Am Chem Soc* 2005; 127:8290-8291.
- [13] Sin SL, Gan LH, Hu X, Tam KC, Gan YY. Photochemical and thermal isomerizations of azobenzene-containing amphiphilic diblock copolymers in aqueous micellar aggregates and in film. *Macromolecules* 2005; 38:3943-3948.
- [14] Yoshida T, Kanaoka S, Aoshima S. Photo-responsive copolymers with azobenzene side groups synthesized by living cationic polymerization: efficient amplification of photosensitivity in aqueous photo-switching system. *J Polym Sci: Part A: Polym Chem* 2005; 43:5337-5342.
- [15] Kadota S, Aoki K, Nagano S, Seki T. Photocontrolled microphase separation of block copolymers in two dimensions. *J Am Chem Soc* 2005; 127:8266-8267.

- [16] Morikawa Y, Nagano S, Watanabe K, Kamata K, Iyoda T, Seki T. Optical alignment and patterning of nanoscale microdomains in a block copolymer thin film. *Adv Mater* 2006; 18:883-886.
- [17] Yu H, Li J, Ikeda T, Iyoda T. Macroscopic parallel nanocylinder array fabrication using a simple rubbing technique. *Adv Mater* 2006; 18:2213-2215.
- [18] Jin M, Lu R, Yang QX, Bao CY, Sheng R, Xu TH, Zhao Y. Preparation of side-on bisazobenzene-containing homopolymers and block copolymers via ATRP and studies on their photoisomerization and photoalignment behaviors. *J Polym Sci: Part A: Polym Chem* 2007; 45:3460-3472.
- [19] Wang D, Ye G, Wang X. Synthesis of aminoazobenzene-containing diblock copolymer and photoinduced deformation behavior of its micelle-like aggregates. *Macromol Rapid Commun* 2007; 28:2237-2243.
- [20] Yu H, Shishido A, Iyoda T, Ikeda T. Novel wormlike nanostructures self-assembled in a well defined liquid crystalline diblock copolymer with azobenzene moieties. *Macromol Rapid Commun* 2007; 28:927-931.
- [21] Su W, Zhao H, Wang Z, Li Y, Zhang Q. Sphere to disk transformation of micro-particle composed of azobenzene-containing amphiphilic diblock copolymers under irradiation at 436 nm. *Eur Polym J* 2007; 43:657-662.
- [22] Breiner T, Kreger K, Hagen R, Häckel M, Kador L, Müller AHE, Kramer EJ, Schmidt H-W. Blends of poly(methacrylate) block copolymers with photoaddressable segments. *Macromolecules* 2007; 40(6):2100-2108.
- [23] He X, Sun W, Yan D, Liang L. Novel ABC2-type liquid-crystalline block copolymers with azobenzene moieties prepared by atom transfer radical polymerization. *Eur Polym J* 2008; 44:42-49.
- [24] Komura M, Watanabe K, Iyoda T, Yamada T, Yoshida H, Iwasaki Y.

- Laboratory-GISAXS measurements of block copolymer films with highly ordered and normally oriented nanocylinders. *Chem Lett* 2009; 38(5):408-409.
- [25] Wang Y, Zhang M, Moers C, Chen S, Xu H, Wang Z, Zhang X, Zhibo L. Block copolymer aggregates with photo-responsive switches: towards a controllable supramolecular container. *Polymer* 2009; 50:4821-4828.
- [26] Khandpur AK, Förster S, Bates FS, Hamley IW, Ryan AJ, Bras W, Almdal K, Mortensen K. Polyisoprene-polystyrene diblock copolymer phase diagram near the order-disorder transition. *Macromolecules* 1995; 28:8796-8806.
- [27] Han CD, Baek DM, Kim JK, Ogawa T, Sakamoto N, Hashimoto T. Effect of volume fraction on the order-disorder transition in low-molecular-weight polystyrene-block-polyisoprene copolymers. 1. Order-disorder transition-temperature determined by rheological measurements. *Macromolecules* 1995; 28:5043-5062.
- [28] Matsen MW, Bates FS. Unifying weak- and strong-segregation block copolymer theories. *Macromolecules* 1996; 29:1091-1098.
- [29] Muthukumar M, Ober CK, Thomas EL. Competing interactions and levels of ordering in self-organizing polymeric materials. *Science* 1997; 277:1225-1232.
- [30] Modi MA, Krishnamoorti R, Tse MF, Wang HC. Viscoelastic characterization of an order-order transition in a mixture of di- and triblock copolymers. *Macromolecules* 1999; 32:4088-4097.
- [31] Abetz V, Goldacker T. Formation of superlattices via blending of block copolymers. *Macromol Rapid Commun* 2000; 21:16-34.
- [32] Lodge TP. Block copolymers: past successes and future challenges. *Macrom Chem Phys* 2003; 204:265-273.
- [33] Yu H, Asaoka S, Shishido A, Iyoda T, Ikeda T. Photoinduced nanoscale

- cooperative motion in a well-defined triblock copolymer. *Small* 2007; 3:768-771.
- [34] Meinhardt R, Macko S, Qi B, Draude A, Zhao Y, Wenig W, Franke H. Photoinduced molecular motion in an azobenzene-containing diblock copolymer. *J Phys D: Appl Phys* 2008; 41:195303 (9 pp).
- [35] Yu H, Naka Y, Shishido A, Ikeda T. Well-defined liquid-crystalline diblock copolymers with an azobenzene moiety: synthesis, photoinduced alignment and their holographic properties. *Macromolecules* 2008; 41:7959-7966.
- [36] Del Barrio J, Oriol L, Alcalá R, Sánchez C. Photoresponsive poly(methyl methacrylate)-*b*-azodendron block copolymers prepared by ATRP and click chemistry. *J Polym Sci: Part A: Polym Chem* 2010; 48:1538-1550.
- [37] Yu HF, Okano K, Shishido A, Ikeda T, Kamata K, Komura M, Iyoda T. Enhancement of surface-relief gratings recorded in amphiphilic liquid-crystalline diblock copolymer by nanoscale phase separation. *Adv Mater* 2005; 17:2184-2188.
- [38] Yu HF, Shishido A, Iyoda T, Ikeda T. Effect of recording time on grating formation and enhancement in an amphiphilic diblock liquid-crystalline copolymer. *Mol Cryst Liq Cryst* 2009; 498:29-39.
- [39] Zhao Y, Ikeda T. *Smart Light-Responsive Materials: Azobenzene-Containing Polymers and Liquid Crystals*, Eds. John Wiley & Sons, Hoboken, New Jersey, 2009.
- [40] Serrano E, Larrañaga M, Remiro PM, Mondragon I, Carrasco PM, Pomposo JA, Mecerreyes D. Synthesis and characterization of epoxidized styrene-butadiene block copolymers as templates for nanostructured thermosets. *Macromol Chem Phys* 2004; 205:987-996.

- [41] Fernández R, Mondragon I, Oyanguren PA, Galante MJ. Synthesis and characterization of epoxy polymers containing azobenzene groups that exhibit optical birefringence. *React Funct Polym* 2008; 68:70-76.
- [42] Ocando C, Tercjak A, Serrano E, Ramos JA, Corona-Galván S, Parellada MD, Fernández-Berridi MJ, Mondragon I. Micro- and macrophase separation of thermosetting systems modified with epoxidized styrene-block-butadiene-block-styrene linear triblock copolymers and their influence on final mechanical properties. *Polym Int* 2008; 57:1333-1342.
- [43] Natansohn A, Rochon P, Gosselin J, Xie S. Azo polymers for reversible optical storage. 1. Poly(4'-((2-(acryloyloxy)ethyl)ethylamino)-4-nitroazobenzene). *Macromolecules* 1992; 25:2268-2273.
- [44] Fernández R, Mondragon I, Galante MJ, Oyanguren PA. Bonding and molecular environment effects on photoorientation in epoxy-based polymers having azobenzene units. *Eur Polym J* 2009; 45: 788-794.
- [45] Fernández R, Mondragon I, Galante MJ, Oyanguren PA. Influence of chromophore concentration and network structure on the photo-orientation properties of crosslinked epoxy-based azopolymers. *J Polym Sci: Part B: Polym Phys* 2009; 47:1014-1014.
- [46] Natansohn A, Rochon P, Pézolet M, Audet P, Brown D, To S. Azo polymers for reversible optical storage. 4. Cooperative motion of rigid groups in semicrystalline polymers. *Macromolecules* 1994; 27:2580-2585.

TABLE CAPTIONS

Table 1. Characteristics of the block copolymers used.

Table 2. FTIR assignments of the relevant absorption bands of the materials used.

Sample	Epoxidation degree (mol %)	PS (wt %)	PB (wt %)	Epoxidized PB (wt %)	AZO (wt %)	T_g PB (°C)
SBS-DO3	0	25	60	0	15	-80 ^a
C500-DO3-PS	0	38	49	0	13	-80 ^a
C500ep11-DO3	11	25	50	10	15	-55

^a Glass transition temperature values for PB/epPB blocks of SBS determined elsewhere [42].

Table 1

Wavenumber (cm ⁻¹)	Band assignment
3500-3400	NH ₂ and NH stretching
3400	OH stretching
3080-3005	C-H stretching of aromatic rings
2920-2840	C-H stretching of aliphatic bonds
1712	C=O stretching

1640	NH ₂ in-plane bending
1600	NH in-plane bending
1640-1600	C=C stretching
1510	NO ₂ asymmetric stretching
1390	N=N stretching
1340	NO ₂ symmetric stretching
1140	C-H stretching
990-910	C=C out-of-plane bending
890	C-O-C asymmetric stretching
855-835	C-H out-of-plane bending of aromatic rings

Table 2

FIGURE CAPTIONS

Figure 1. Synthesis of azo-containing block copolymers.

Figure 2. ¹H NMR spectra of parent copolymers, (a) C500 and (b) C540, and epoxidized copolymers, (c) C500ep11 and (d) C540ep14.

Figure 3. FTIR spectra of DO3, C500ep11, and C500ep11 and C500ep11-DO3 after annealing at 110 °C for 24 h within the range: (a) 3600-800 cm⁻¹ and (b) 1700-800 cm⁻¹.

Figure 4. TM-AFM phase image (left) and profile (right) of C500-DO3 after annealing at 110 °C for 24 h ($3\ \mu\text{m} \times 3\ \mu\text{m}$). The straight line on the image indicates the position where the profile was measured.

Figure 5. TM-AFM phase image (left) and profile (right) of C500-DO3-PS after annealing at 110 °C for 24 h and 210 °C for 4 min ($3\ \mu\text{m} \times 3\ \mu\text{m}$). The straight line on the image indicates the position where the profile was measured.

Figure 6. TM-AFM phase images of (a) C500ep11-DO3 and (b) C540ep14-DO3 after annealing at 110 °C for 24 h, and (c) C500ep11-DO3 and (d) C540ep14-DO3 after annealing at 110 °C for 48 h ($2\ \mu\text{m} \times 2\ \mu\text{m}$).

Figure 7. Writing-relaxing curves of (a) C500-DO3, (b) C540-DO3, (c) C540-DO3-PS, (d) C500ep11-DO3, and (e) C500ep11-DO3 and (f) C540ep14-DO3 after annealing at 110 °C for 24 h. The writing beam is on at point A and off at B.

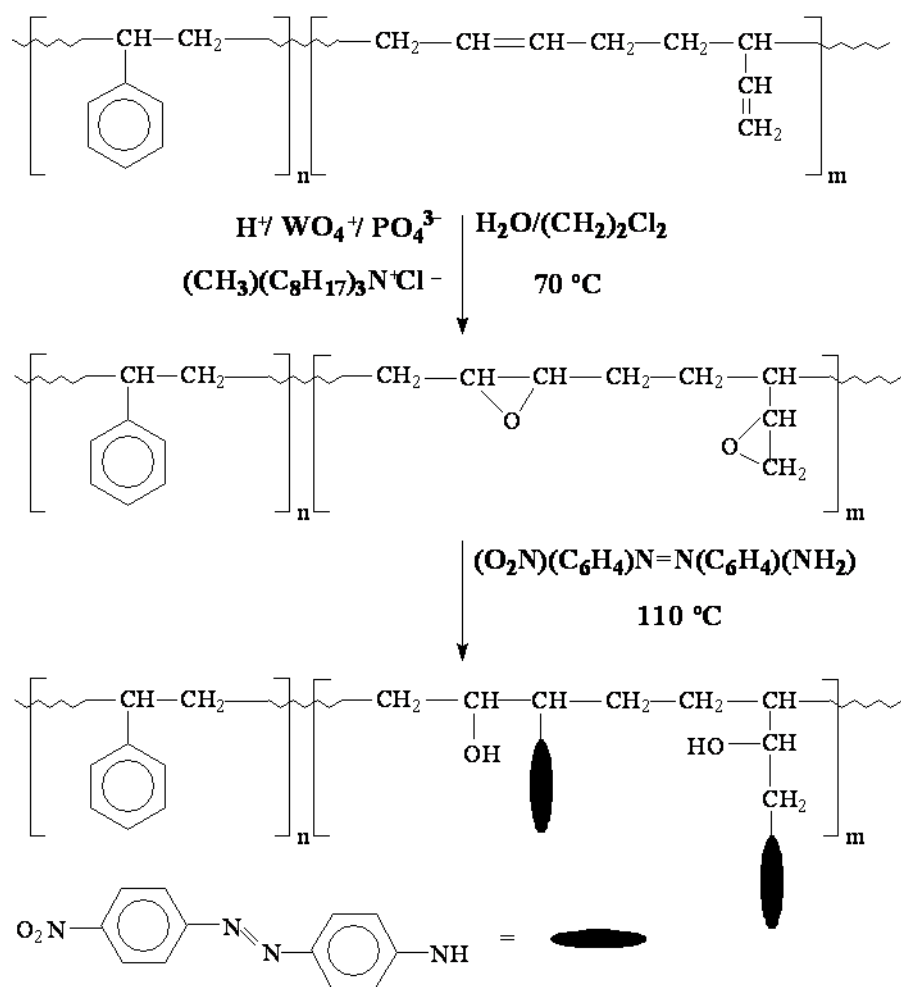


Figure 1

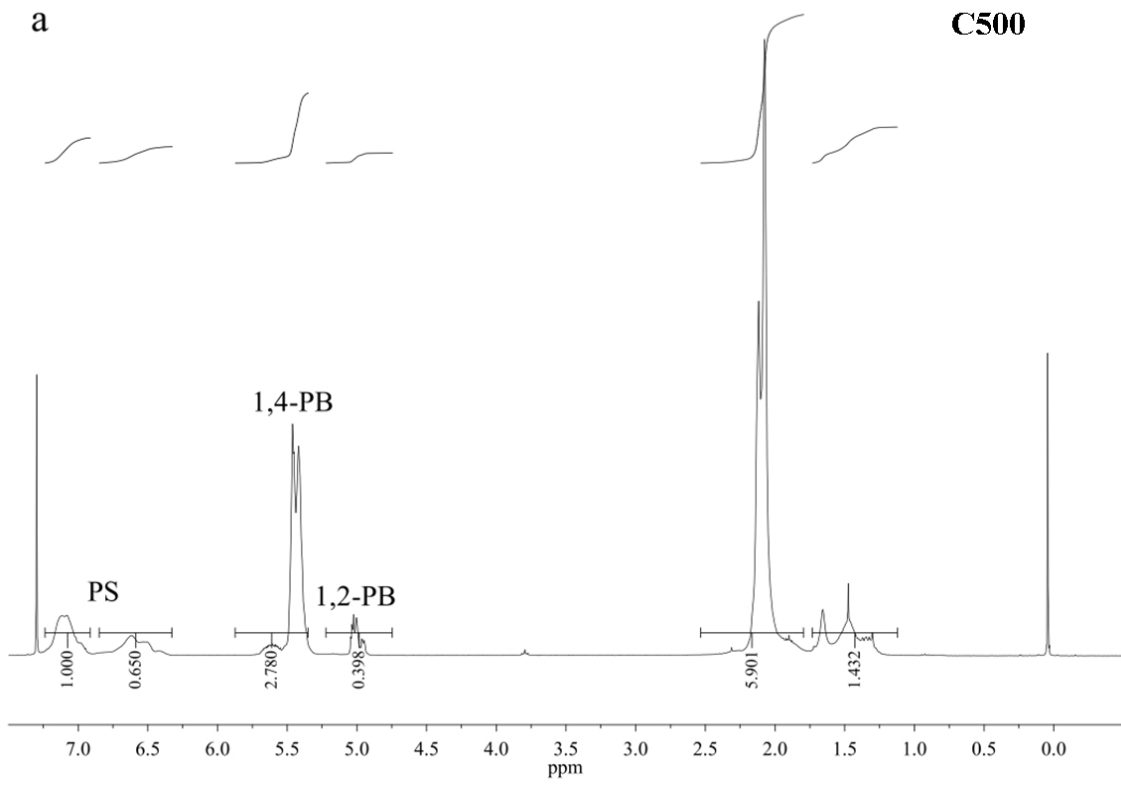


Figure 2a

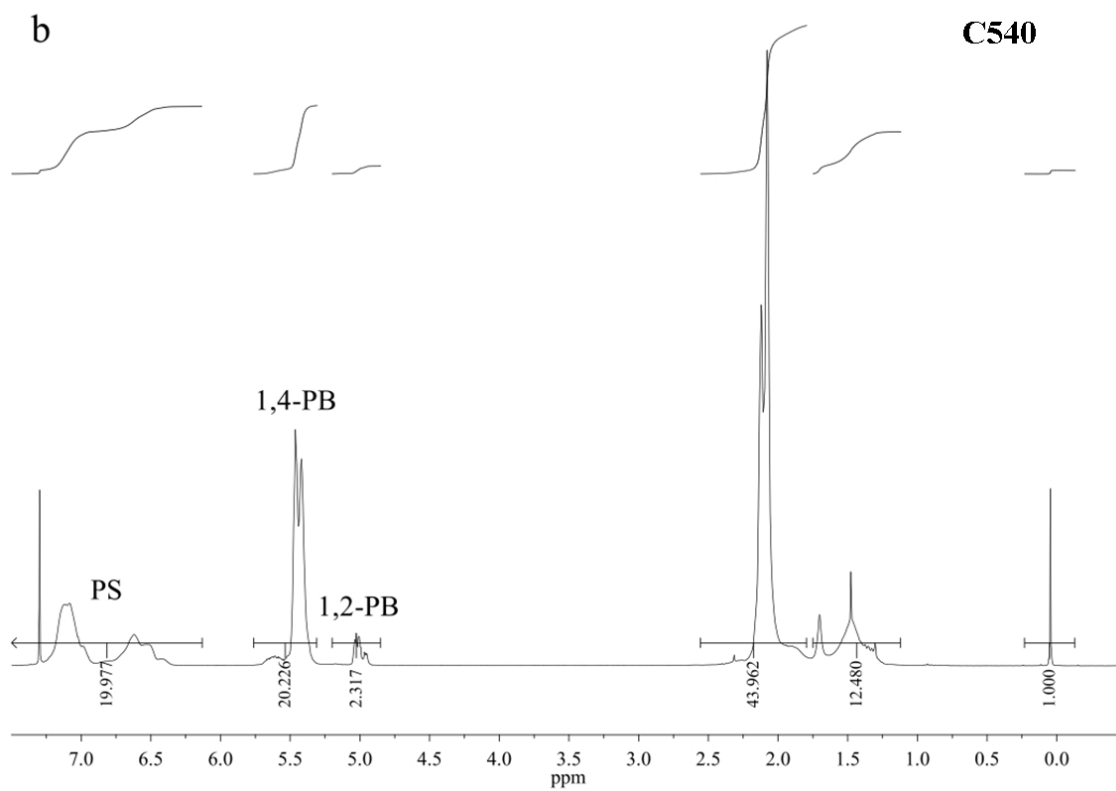


Figure 2b

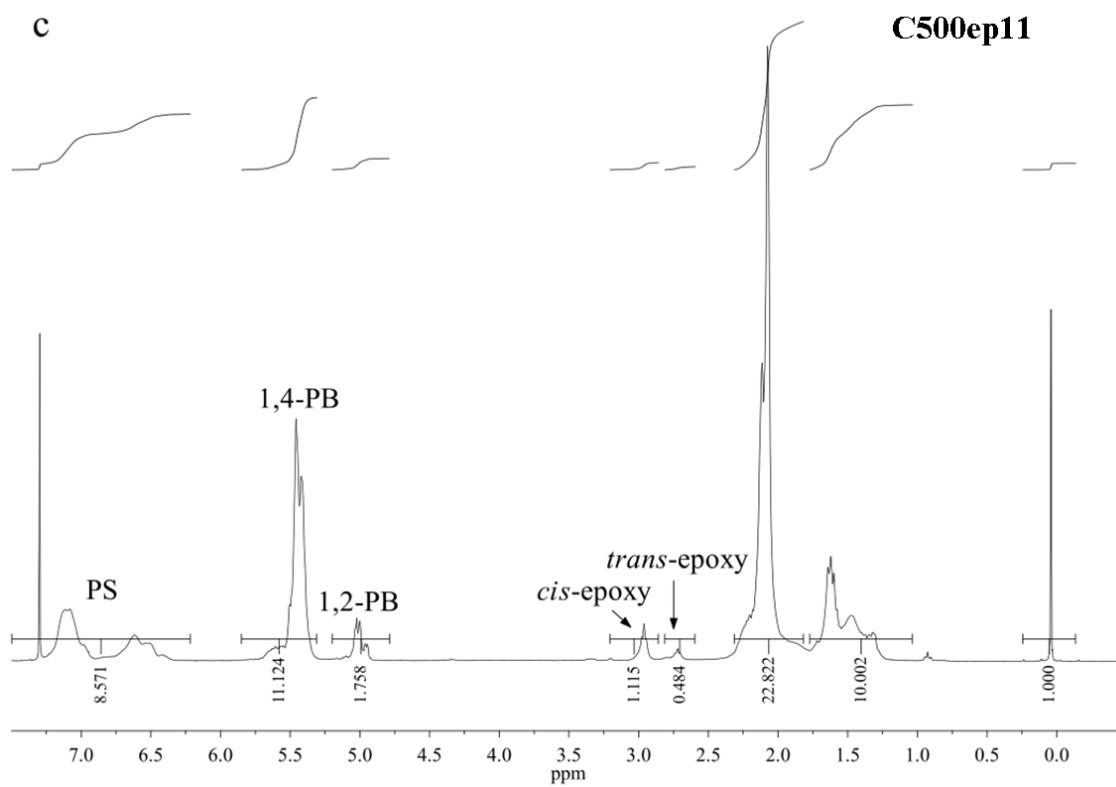


Figure 2c

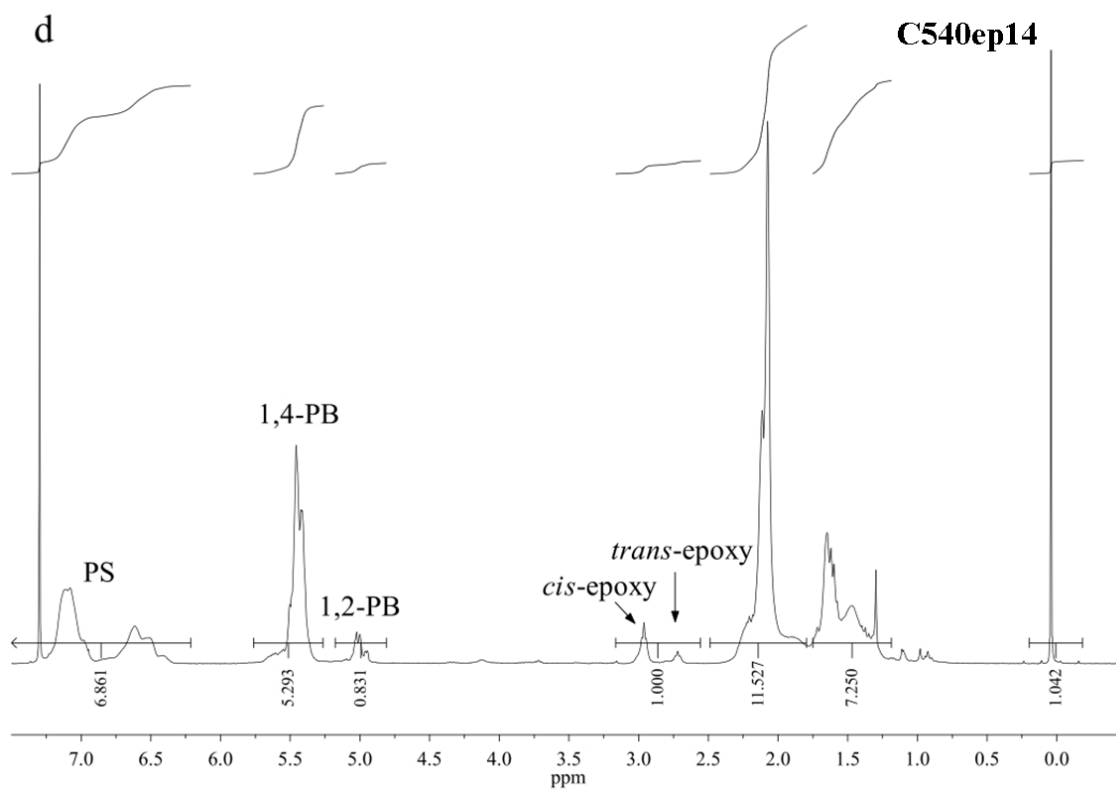


Figure 2d

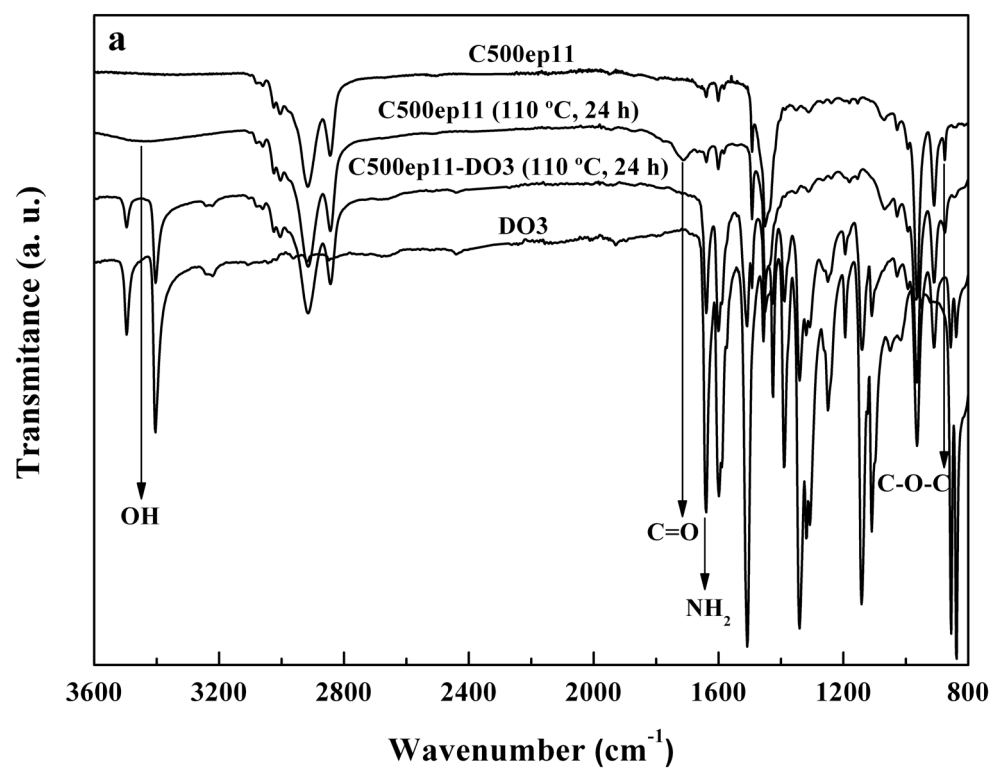


Figure 3a

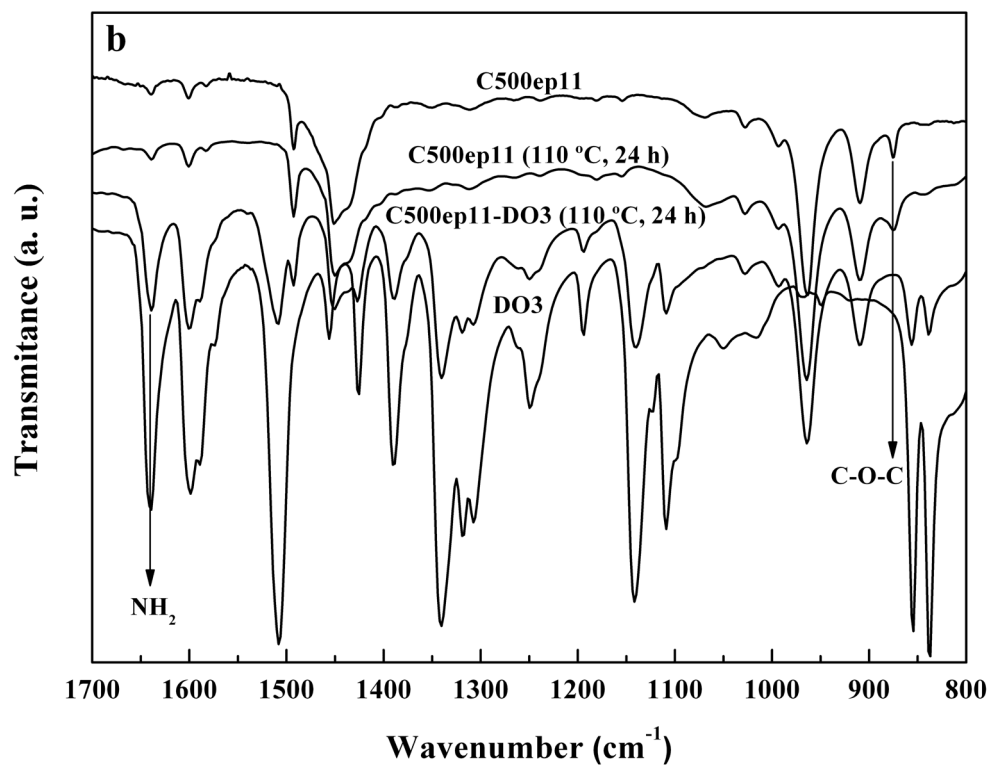


Figure 3b

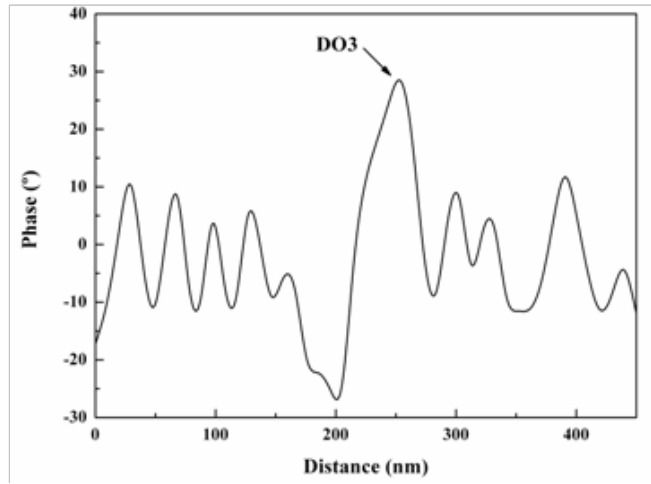
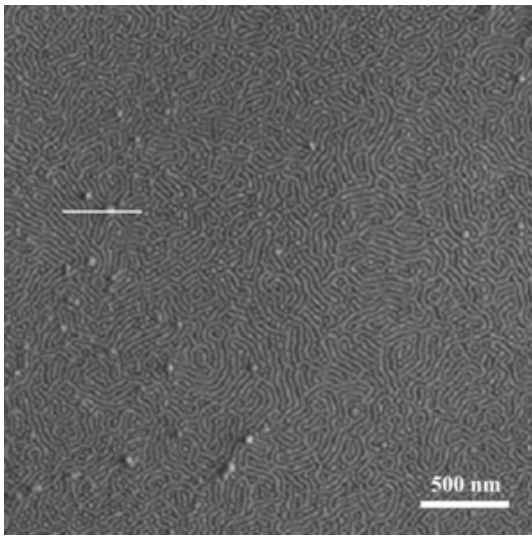


Figure 4

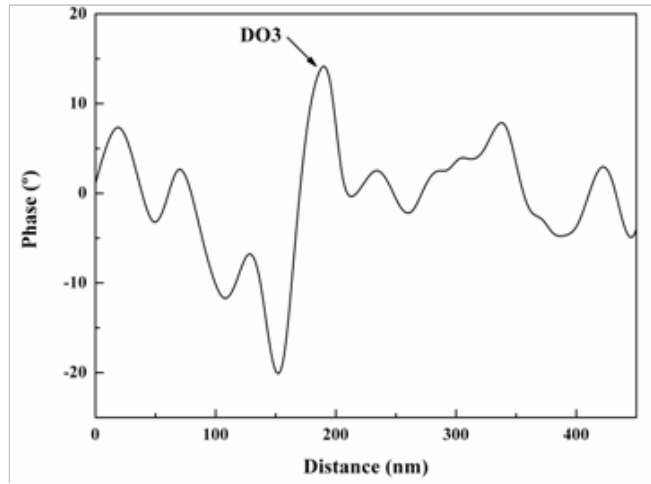
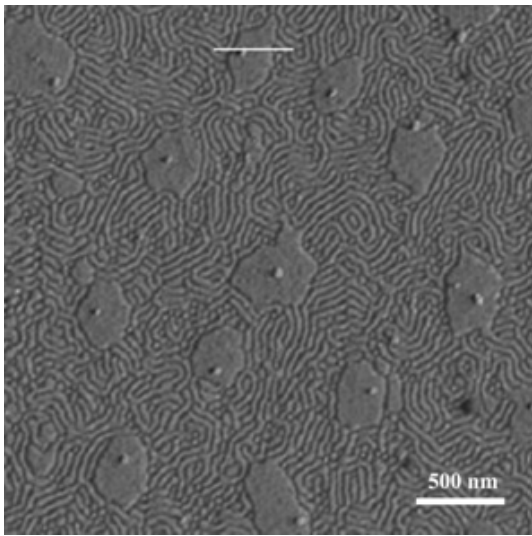


Figure 5

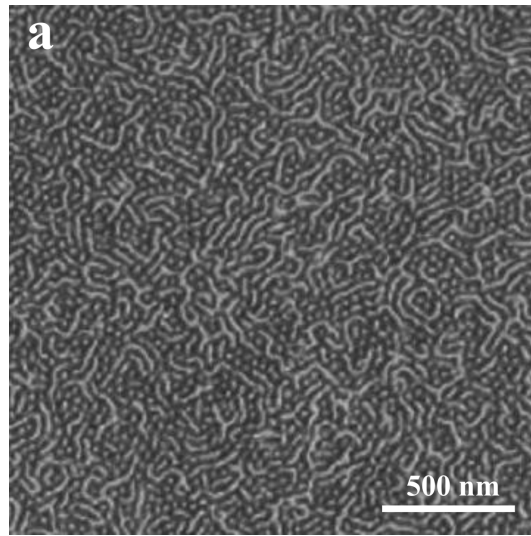


Figure 6a

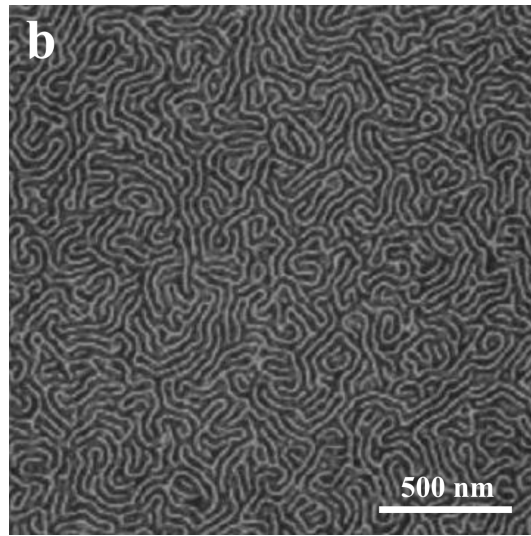


Figure 6b

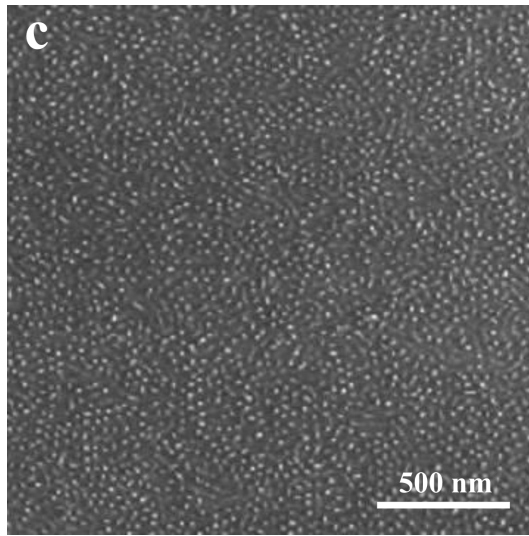


Figure 6c

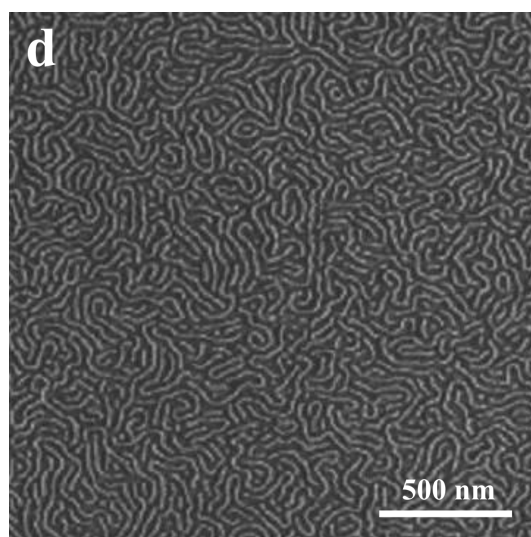


Figure 6d

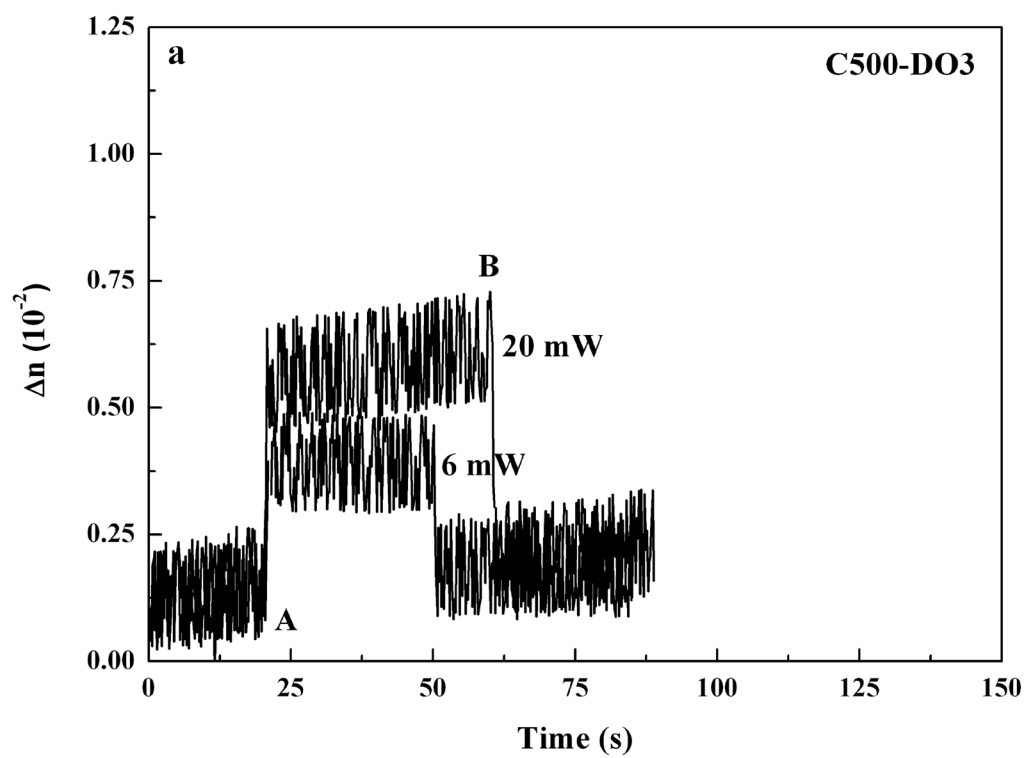


Figure 7a

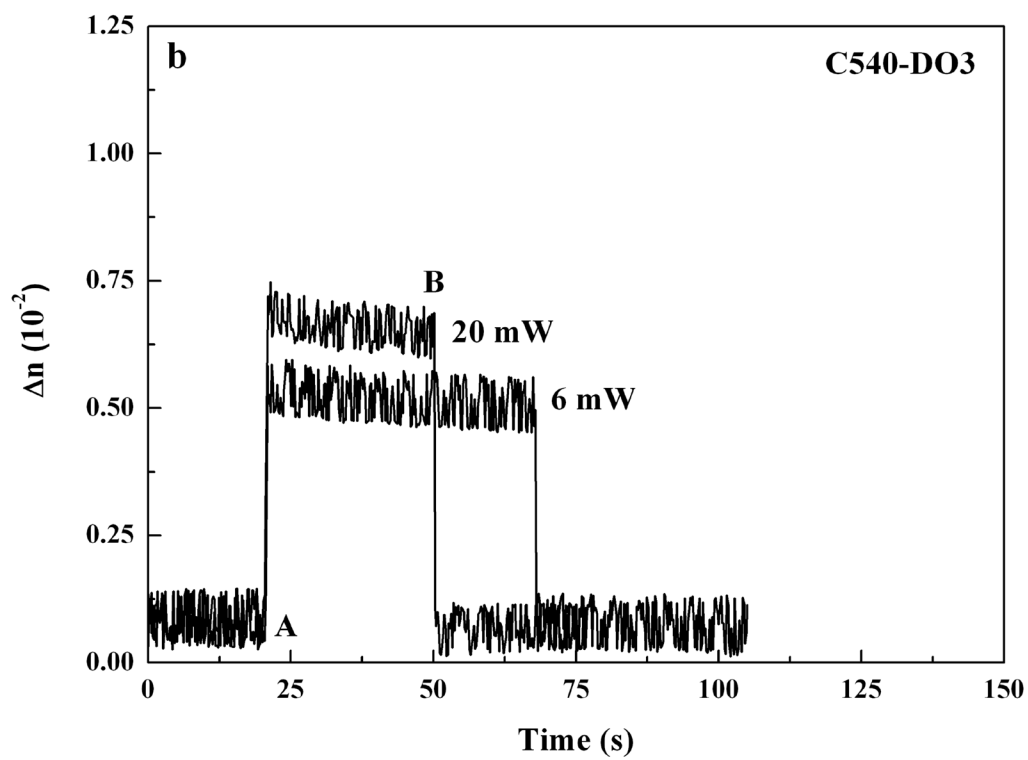


Figure 7b

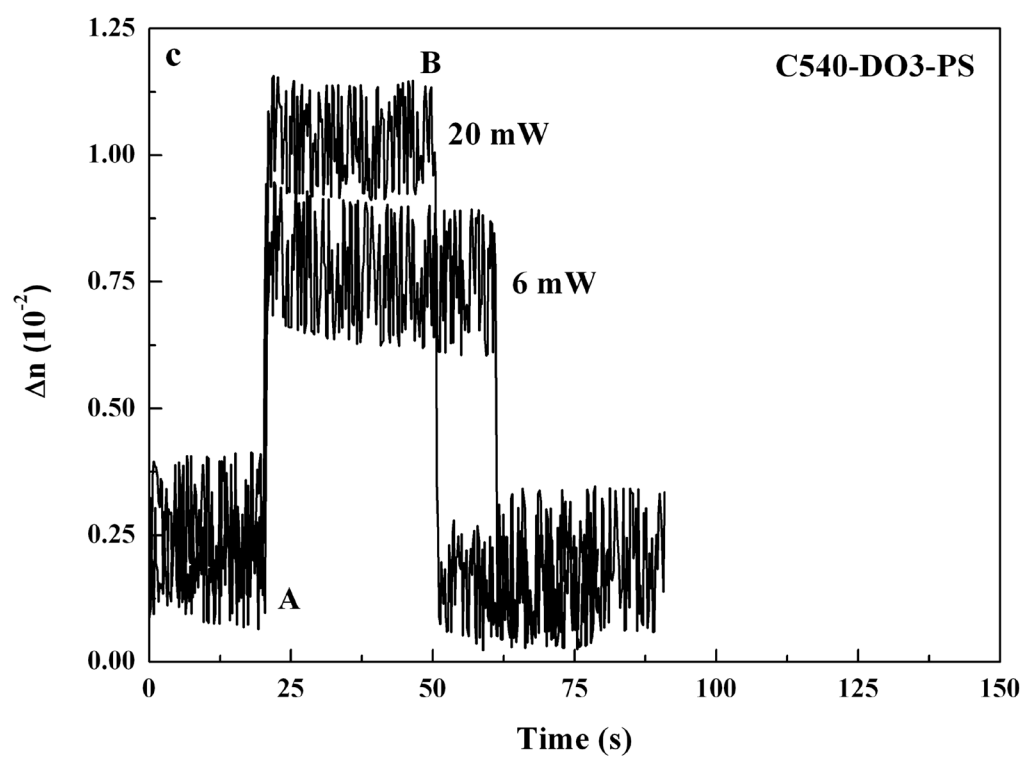


Figure 7c

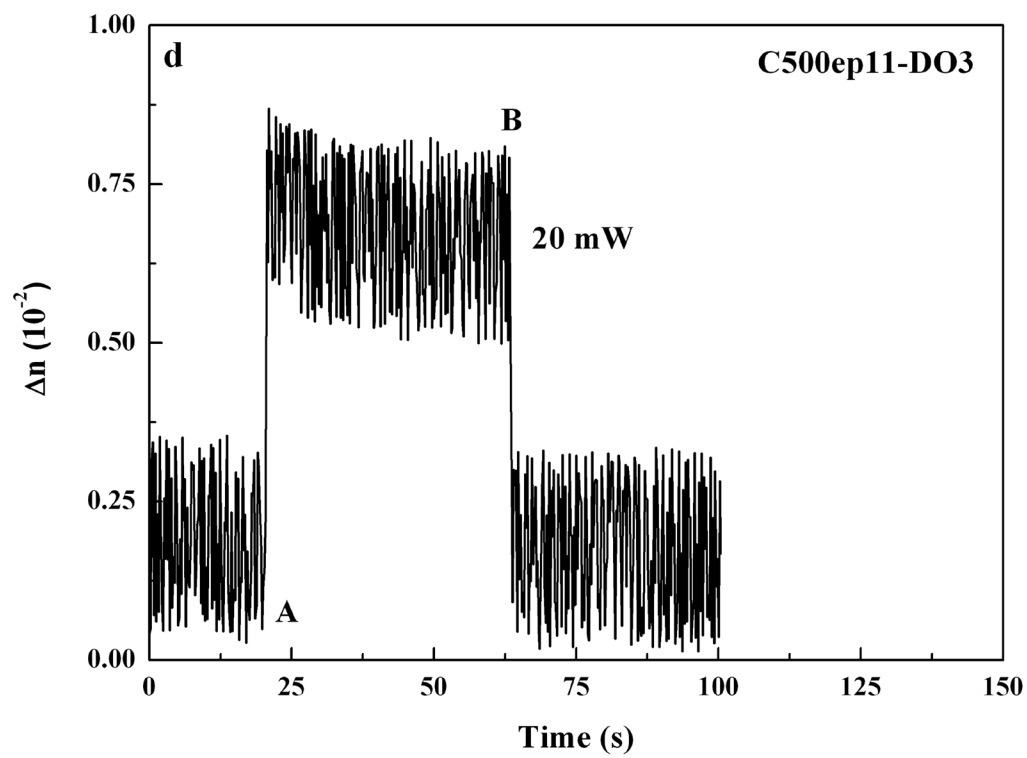


Figure 7d

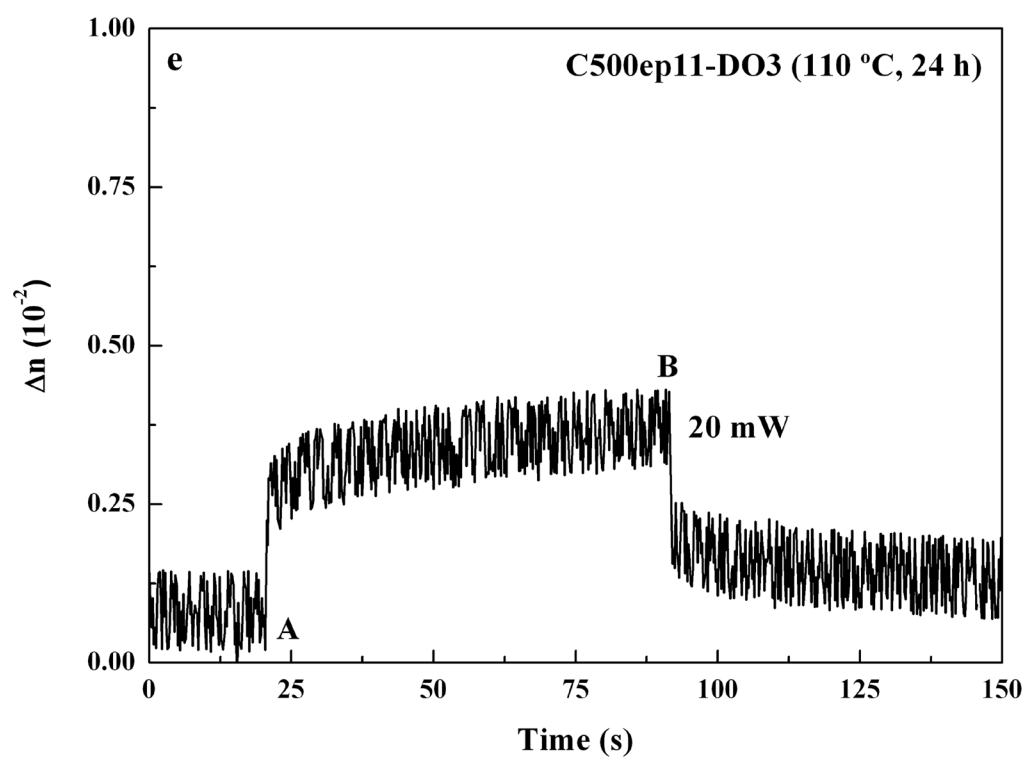


Figure 7e

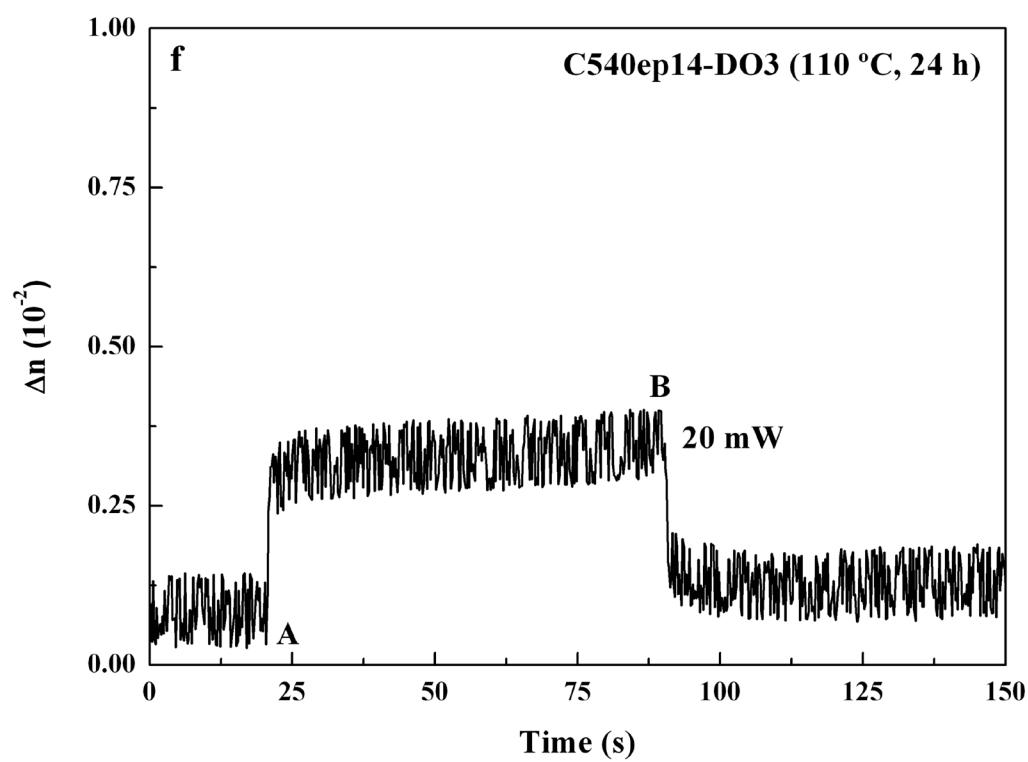


Figure 7f